Hindawi Publishing Corporation
Advances in Materials Science and Engineering
Volume 2016, Article ID 7868194, 12 pages
http://dx.doi.org/10.1155/2016/7868194

Research Article

The Effect of Salt Solutions and Absorption Cycles in the Capillary and Drying Coefficient of Red Brick Samples with Different Joints

A. S. Guimarães, J. M. P. Q. Delgado, V. P. de Freitas, and A. P. Albuquerque

CONSTRUCT-LFC, Faculty of Engineering, University of Porto, Rua Dr. Roberto Frias, s/n, 4200-465 Porto, Portugal

Correspondence should be addressed to J. M. P. Q. Delgado; jdelgado@fe.up.pt

Received 27 January 2016; Accepted 22 March 2016

Academic Editor: Luigi Nicolais

Rising damp can reduce building's aesthetical value, comfort, and health mark when combined with the existence of soluble salts in the building components and in the ground water can even lead to material decomposition and compromise its structural performance. This research work intended to study the effect of different absorption cycles of two saturated solutions of sodium sulphate and potassium chloride in the capillary absorption curves obtained through the partial immersion of red brick samples without and with different joints. The results revealed significant differences in the capillary coefficients obtained when samples were tested with salt solutions. In the end of this paper an evaluation of the drying kinetics was presented for all the tested samples. Four different first-order kinetics models, available in the literature, were adjusted to describe the drying process and the results point that the Page and Logarithmic models allow the best fit. The apparent molecular diffusion coefficient for solid red brick samples saturated with different solutions and joints was also estimated.

1. Introduction

Rising damp is one of construction's major problems especially in old, ancient, and historical buildings associated porous materials used in this industry. This happens due to the migration of the salt ions dissolved in water into the porous network of the building's walls where they remain and crystalize after water evaporates, dealing great pressures against the pore walls and eventually resulting in their fracture after many cycles of crystallization/dissolution [1, 2]. This mechanism has a massive influence on the degradation of historical buildings since they were built in a time when construction technologies made no effort to prevent this kind of pathologies.

The materials used in the construction industry exhibit porous characteristics that favour the moisture fixation through mechanisms like capillary, hygroscopicity, and condensation [3–7]. The experiments reported in this paper are directly related to rising damp, one of the moisture propagation phenomena that cause further deterioration in buildings. Rising damp may be explained by the capillary migration of water from the soil through the porous network of the materials that compose building elements. This kind of damp assumes a greater expression in old buildings, mostly constructed in masonry, in which porous materials such as ceramic bricks, mortars, and stones are used [1, 2].

The presence of dissolved salts in the water, which uprises through the porous network of building elements, constitutes an annoying factor for its degradation [8, 9]. If, on one hand, salts follow the water during its rise in liquid phase, the same does not occur when the water evaporates. Therefore, the salts remain in the porous structure of the building materials and eventually crystallize after the solution has reached its supersaturation state. Salt can crystallize on the surface of the materials developing efflorescence with aesthetical consequences for the building or inside the porous structure, inflicting great pressures over the pore walls that can disintegrate them when surpassing its mechanical resistance [10, 11]. Hygrothermal oscillation of the surrounding environment may promote cycles of crystallization/dissolution and potentially developing wrecking tensions in different pores in each cycle.

Adding to this, the constructive systems, elements, and components, particularly the masonry, base their functional efficiency on the combination of materials with different characteristics. However, this heterogeneity makes moisture transfer analysis much more complex, demanding the knowledge, not only about the individual characteristics of the materials but also about the continuity conditions of the interface that separates the distinct materials and that is why the knowledge about the joints influence in those transport phenomena is considered crucial [12–14].

This paper intends to report the experimental work carried out with brick specimens, aiming to evaluate the effect of salt solutions in the capillary absorption of monolithic brick specimens in comparison with water. Sodium sulphate and potassium chloride were the chosen salts to perform the experiments. The first is one of the salts that impose more degradation to buildings; the second was chosen for being very commonly found in building materials, especially the ion chloride. It also presents the drying kinetics and five models were adjusted to describe the drying process. Finally, in the capillary absorption and drying tests, different joints as perfect contact (just in contact), hydraulic continuity (with interpenetration of both materials), and air space (with an air layer between different materials) were also tested to evaluate the interface effect in moisture transference processes.

2. Materials and Methods

The test specimens used were nine red brick monolithic samples with the dimensions $5 \times 5 \times 10\,\text{cm}^3$ (three for each solution including water). All the specimens were sealed in the lateral faces with an epoxy coating to avoid the evaporation through these sides and assure the unidirectional moisture flow from the bottom to the specimens' top surface. Tests were performed only for pure water and two saturated salt solutions (KCl and Na_2SO_4). The solutions were saturated with salt excess in order to avoid the decrease of ions during the absorption process.

2.1. Capillary Coefficient. The capillary absorption tests followed the procedure n° II.6 "Water Absorption Coefficient (Capillary)" of RILEM [15]. The tests were preceded by the drying of the specimens in an oven at about 60°C until obtaining constant mass, in order to calculate the dry mass of the specimens. After this step, specimens were stored in the test room for some days, until they reach the hygrothermal equilibrium.

Mukhopadhyaya et al. [16] confirmed the temperature influence on capillary absorption coefficient of brick specimens in their study with different porous materials. In order to minimize the effect of temperature on our results, tests were performed in a room with controlled temperature. The values of temperature and relative humidity (RH) of the air were measured every ten minutes for 33 days using a sequential data recording device. The mean values obtained were 22.8°C for the temperature and 52.7% for the RH.

Tests began with the partial immersion of the specimens 5 mm deep. After the immersion, weightings were performed periodically in order to determine the amount of water absorbed during the test. On the first day, weightings were performed on all samples at minutes 1, 3, 5, 10, 15, 30, and 60 and afterwards at least once an hour. In general, weightings were attempted every two hours on the second day, every three hours on the third day, and once a day for the remaining days of testing. This timing had yet to suffer some adjustments for some combinations tested. For instance, for the specimens with air space between layers, after the wet front has reached the interface the time between weightings was extended since the moisture transport at the interface took place in the vapor phase and was therefore much slower.

The amount of absorbed water per unit area at time t assay M_w (kg/m^2) is calculated using (1), where M_0 (kg) is the dry mass of the sample, M_i (kg) is of the mass of sample at time t, and A (m^2) is the area of the base of the specimen:

$$M_w = \frac{M_i - M_0}{A}. \tag{1}$$

Once the amount of water absorbed over the time until the saturation of the porous media was determined, it was then possible to calculate the capillary absorption coefficient, A_w, and the maximum moisture flow through the interface. The earlier one corresponds to the slope of the first linear portion of the imbibition curve that expresses the amount of water absorbed per unit area (kg/m^2) as a function of the root of time (s$^{1/2}$). The second corresponds to the slope of the linear approximation of the imbibition curve that expresses the amount of water absorbed per unit area (kg/m^2) as a function of time (s) once reached the interface.

The results of capillary absorption are given by the sorptivity S (m/s$^{0.5}$). This property, which depends on both the material and the liquid, expresses the tendency of a building material to absorb and transmit a liquid by capillarity [6], as shown by

$$S = \left(\frac{\sigma}{\eta}\right)^{1/2} \dot{S}, \tag{2}$$

where σ is the surface tension of the liquid, η is the viscosity of the liquid, and S is the intrinsic sorptivity of the material. It is important to be in mind that the relation between capillary absorption coefficient and sorptivity is given by $A_w = S \cdot \rho_w$, where ρ_w is the water density (kg/m^3).

2.2. Drying Kinetics. Drying was assessed following the experimental procedure of RILEM [15]. It consists in soaking the specimens and then letting them dry through their top surface under controlled environmental conditions. Meanwhile, the loss of water is monitored by periodical weighing. The results are expressed by the so-called mass drying curve which depicts the variation in moisture content over time.

Frequently, quite simple models [17, 18] are presented to describe the drying curves that can provide an adequate representation of the experimental results. One of the most simplified models is the exponential model:

$$\text{MR} = \frac{w - w_e}{w_0 - w_e} = e^{-kt}, \tag{3}$$

Table 1: Mathematical models given by various authors for drying curves.

Model equation	Model name
$MR = e^{-kt}$	Exponential
$MR = e^{-kt^n}$	Page
$MR = a \times e^{-kt} + b$	Logarithmic
$MR = a \times e^{-kt^n} + b \times t$	Midilli et al.

where w is the average moisture content at any time, w_0 is the initial moisture content, w_e is the equilibrium moisture content, k is the drying rate constant, and t is the drying time. Usually, this model does not provide an accurate simulation of drying curves of many building materials, underestimating the beginning of the drying curve and overestimating the later stages. To soften this minor accuracy, the Page model is applied with an empirical modification to the time term by introducing an exponent, n:

$$\mathrm{MR} = \frac{w - w_e}{w_0 - w_e} = e^{-kt^n}. \tag{4}$$

These empirical models derive a direct relationship between average moisture content and drying time. However, they neglect the fundamentals of the drying process and their parameters have no physical meaning.

In this work, the drying curves were fitted with four different empirical and semiempirical drying models (see Table 1). Regression analyses of these equations were done by using STATISTICA routine. The regression coefficient (R^2) was primary criterion for selecting the best equation to describe the drying curves of ETICS. The performance of derived new models was evaluated using various statistical parameters such as the mean bias error (MBE), the root mean square error (RMSE), and chi-square (χ^2), in addition to the regression coefficient (R^2). These parameters can be calculated as follows:

$$\mathrm{MBE} = \frac{1}{N}\sum_{i=1}^{N}\left(\mathrm{MR}_{\mathrm{pre},i} - \mathrm{MR}_{\mathrm{exp},i}\right), \tag{5a}$$

$$\mathrm{RMSE} = \sqrt{\frac{1}{N}\sum_{i=1}^{N}\left(\mathrm{MR}_{\mathrm{pre},i} - \mathrm{MR}_{\mathrm{exp},i}\right)}, \tag{5b}$$

$$\chi^2 = \frac{\sum_{i=1}^{N}\left(\mathrm{MR}_{\mathrm{exp},i} - \mathrm{MR}_{\mathrm{pre},i}\right)^2}{N - p}. \tag{5c}$$

The mechanisms of mass transfer in building materials are complex and frequently the modelling of the drying curves during the falling rate period is carried out by assuming that the main mechanism is of diffusional nature. In accordance with this, the experimental drying data for determination of apparent molecular diffusion coefficient was interpreted by using Fick's diffusion model. In a one-dimensional formulation with the diffusing substance moving in the direction normal to a sheet of medium of thickness L, the diffusion equation can be written as [19]

$$\frac{\partial w}{\partial t} = D_{\mathrm{eff}}\frac{\partial^2 w}{\partial x^2} \tag{6}$$

subject to the following boundary conditions:

$$\begin{aligned} &t = 0, \\ &0 < x < \infty, \end{aligned} \tag{7a}$$

$$w = w_0,$$

$$\begin{aligned} &t > 0, \\ &x = 0, \end{aligned} \tag{7b}$$

$$w = w_e,$$

$$\begin{aligned} &t > 0, \\ &x \longrightarrow \infty, \end{aligned} \tag{7c}$$

$$w = w_0.$$

The analytical solution of (6) with the initial and boundary conditions (7a)–(7c) is

$$\mathrm{MR} = \frac{w - w_0}{w_e - w_0} = 1 - \mathrm{erf}\left(\frac{x}{2\sqrt{D_{\mathrm{eff}}t}}\right). \tag{8}$$

Integrating in respect of t the rate of the penetration of sample face unit area ($x = 0$) by water vapor, the total amount of diffusing substance in time t is obtained; then the appropriate solution of the diffusion equation (8) may be written as follows:

$$\mathrm{MR} = \frac{8}{\pi^2} \times \sum_{n=0}^{\infty}\frac{1}{(2n+1)^2}\exp\left[-(2n+1)^2\pi^2\frac{D_{\mathrm{eff}}t}{L^2}\right] \tag{9}$$

and for long drying times (neglecting the higher order term by setting $n = 0$) it has been simplified as follows:

$$\ln(\mathrm{MR}) = \ln\left(\frac{8}{\pi^2}\right) - \left[\pi^2\frac{D_{\mathrm{eff}}t}{L^2}\right]. \tag{10}$$

3. Results and Discussion

3.1. Capillary Coefficient. Figure 1 sketches a representation of the monolithic specimen, hydraulic continuity interface, perfect contact interface, and air space interface.

The capillary absorption curves obtained in those specimens for each one of the three solutions tested are represented in Figures 2 and 3. The capillary absorption coefficients determined from these curves are represented in Table 2.

The results exposed in this paper regarding the capillary absorption coefficient support the hypothesis that the presence of soluble salts dissolved in water influences the wetting kinetics of porous materials, at least of brick material as it

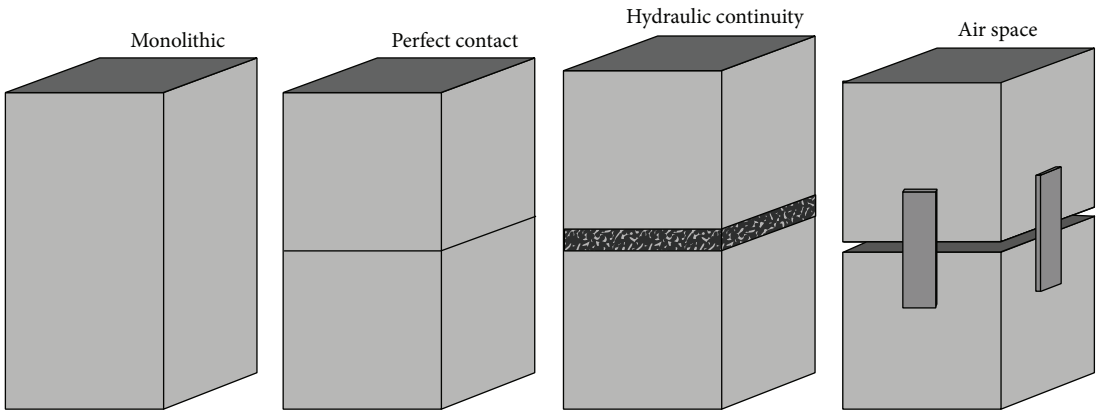

Figure 1: Virtual representation of the different types of specimen tested.

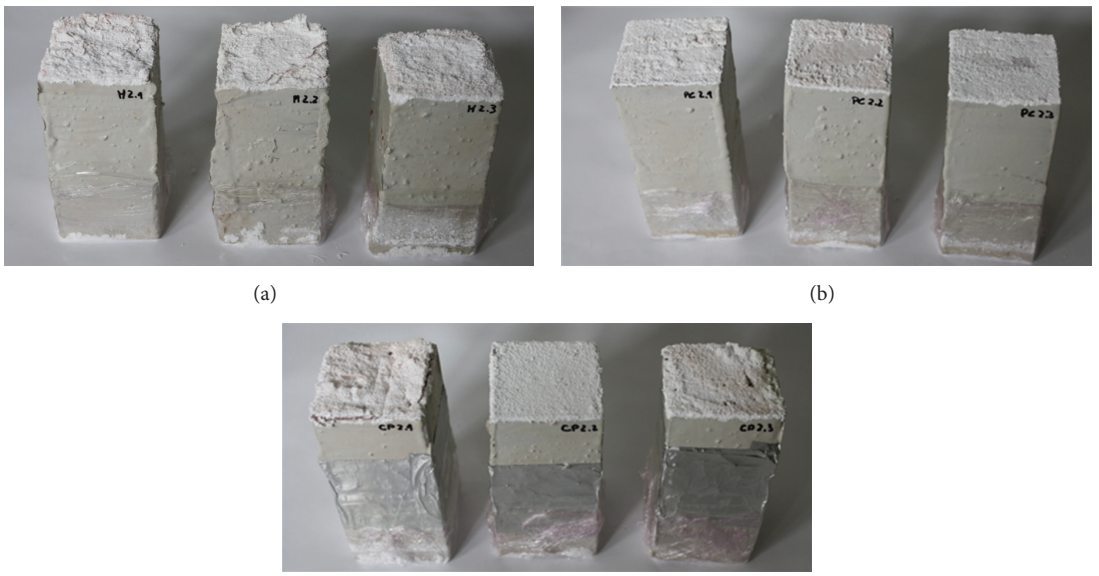

Figure 2: Illustration of some samples before the beginning of the 2° cycle tests: (a) monolithic specimens, (b) hydraulic continuity interface, and (c) perfect contact interface.

was the porous material in study. The capillary absorption coefficient determined for the specimens immersed in saturated solution of sodium sulphate was way lower than the one obtained for the reference test (pure water). On the other hand, potassium chloride appears to induce an increase in this coefficient in comparison with the reference solution. However, the difference between the capillary absorption coefficient of sodium sulphate solution and the reference solution is higher than the one between the potassium chloride and the latter. Our results are in line with that observed by Azevedo [11] who concluded that salts with potassium ion (K^+) lead to the decrease of the capillary absorption coefficient when compared with pure water, while salts with sodium ion (Na^+) induce a decrease in the capillary absorption coefficient.

In Figure 4 it is possible to see the capillary absorption curve of red brick samples as a function of the root of time, after 1 and 2 cycles, with pure water and saturated solutions of KCl and Na_2SO_4, for each joint type. A more detailed analysis was done in Figure 5, and the results obtained show that comparing the 1st and 2nd absorption cycles, it is possible to conclude that the specimens immersed in water practically absorbed the same amount of water, but when the samples are immersed in salt solutions (Na_2SO_4 and KCl) the mass gain in the absorption process is lesser in the 2nd cycle than in the 1st cycle.

Figure 6 shows the mass gain by the samples tested in water and both salts solutions, for the three different joints analysed. For hydraulic continuity interface, the contact between layers was done with a mortar joint of 3 mm and with an interpenetration of both layers. Figure 6 shows slowing of the wetting process when the moisture reaches the interface due to the interface hygric resistance. This result reveals the existence of a resistance associated with the maximum

(a)

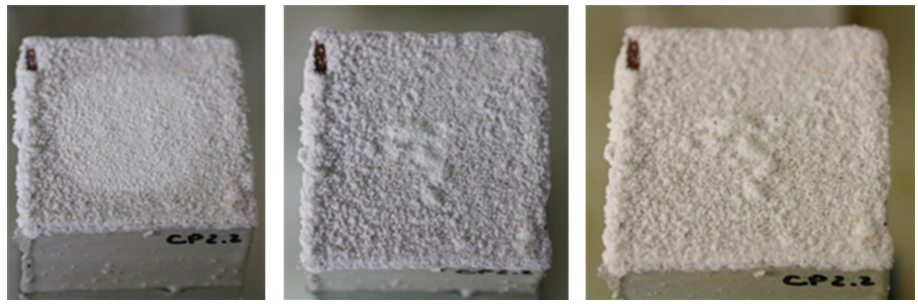

(b)

Figure 3: Illustration of some samples after several weeks of the 2° cycle tests: (a) monolithic specimens and (b) perfect contact interface.

Table 2: Capillary absorption coefficient of monolithic red brick specimens partially immersed in pure water and saturated solutions of KCl and Na_2SO_4.

Solution	Capillary absorption coefficient [kg/(m^2·s$^{1/2}$)]		
	Mean	Standard deviation	Variation coeff (%)
Water	0.0675	0.0035	5.2%
Water + Na_2SO_4	0.0551	0.0025	4.5%
Water + KCl	0.0660	0.0025	10.6%

flow transmitted (FLUMAX) that presents the higher value FLUMAX, as showed in Figure 7. The maximum flow transmitted value is a parameter easy to obtain experimentally and an important input for the hygrothermal programs available in literature [20].

In the situation of perfect contact interface, the experiments detailed in Figure 6 show slowing of the wetting process when the moisture reaches the interface due to the interface hygric resistance. Once again, this result reveals the existence of resistance associated with the maximum flow transmitted, but the lower slow mass gain by the samples indicates a high hygric resistance and an expectable lower maximum flow transmitted value than the obtained one in the hydraulic continuity interface situation.

Finally, for the samples with air space interface, the samples are separated by about 3 mm of an air space in order to have hydric cut that prevents the moisture transfer in liquid phase. Figure 6 shows a slowing of the wetting process when the moisture reaches the interface due to the interface hygric resistance; however, this hygric resistance is higher than the resistance observed in the perfect contact interface. This phenomenon is observed by the extremely slow weight gain presented in Figure 6, for the situation described, and once again reveals the existence of resistance associated with the maximum flow transmitted. This value is expected to be lower than the obtained one with a perfect contact interface (see Figure 7).

3.2. Drying Kinetics. Figure 8 shows the changes in the moisture variation with time during the drying process for different joints and liquid solutions. The common feature of the curves seen in Figure 8 is their similarity as being typical drying curve, as moisture content decreased exponentially with time.

Drying rate decreases continuously with time and decreasing moisture content. This result shows that dominant physical mechanism governing moisture movement in red brick samples is the second drying stage. During the second stage of the drying process the diffusion within the building material limits the rate of evaporation.

Five drying models have been used to describe drying curves and the applicability of these models is presented in Tables 3 and 4. The criterion used for selecting the models that better describe the drying process was the magnitude of

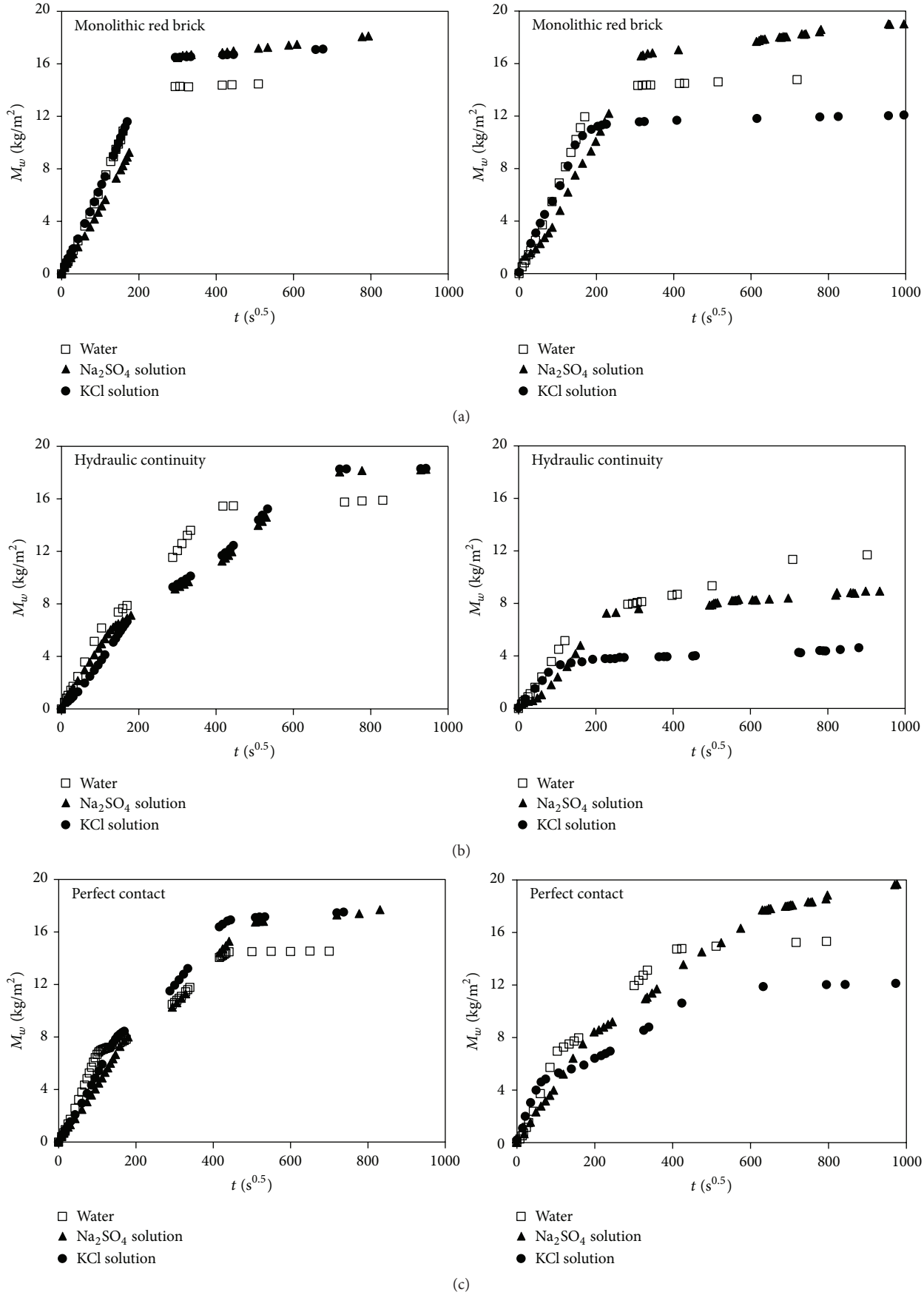

Figure 4: Continued.

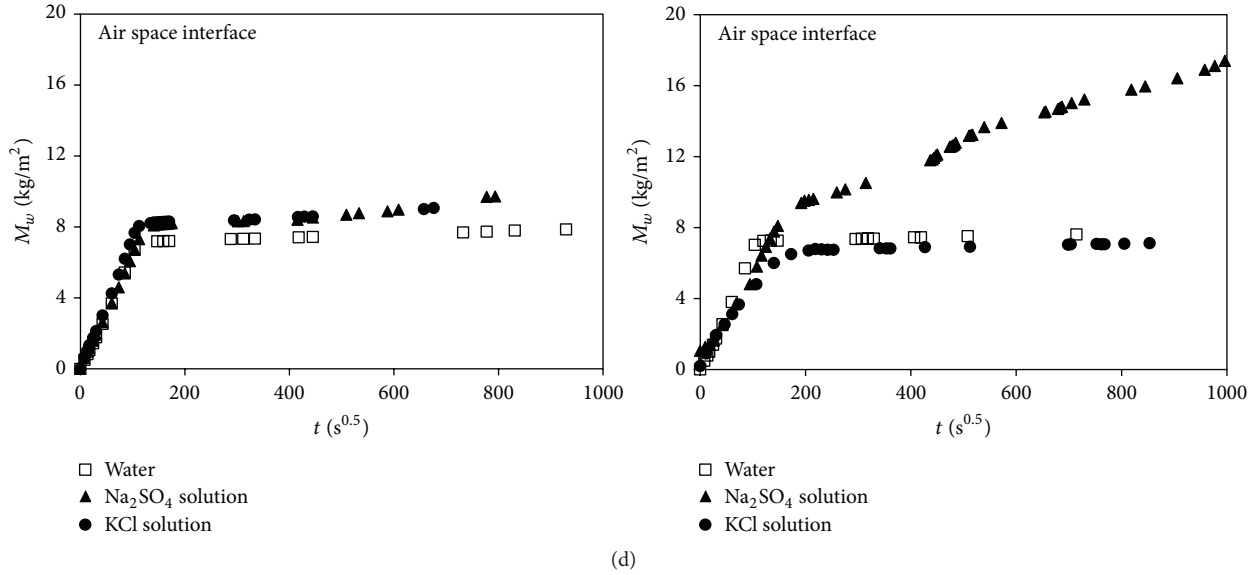

(d)

Figure 4: Capillary absorption curve of red brick samples as a function of the root of time, after 1 and 2 cycles, with pure water and saturated solutions of KCl and Na_2SO_4, for (a) monolithic specimens, (b) hydraulic continuity interface, (c) perfect contact interface, and (d) air space interface.

the relative error for each one (see Table 4). The Page and Logarithmic models presented the best results.

The results reported in Table 3 show that the drying constant obtained is greater for red brick samples with pure water than with the salt solution analysed. It is important to be in mind that with salt solutions the drying process is more complex considering the salt ions stays in the material and the difficult transport process. Another important conclusion is the influence of the joints in the drying process, and it is possible to observe that the monolithic samples and the samples with perfect contact present higher values of drying constant than the samples with hydraulic continuity. Figure 8 also shows that monolithic samples and samples with perfect contact interface present a similar drying process, which should be expected due to the nature of the perfect contact joint. The samples with air space interface present the higher drying constant value which, considering the highest contact with air that they have, to eliminate water, seems to be expected and a realistic result.

Finally, in order to establish the diffusional model, the effective diffusivity coefficient was identified by using (9) and the experimental drying curves of red brick samples were obtained. Effective diffusivity coefficient determination results from plot of dimensionless moisture ratio which is obtained from experimental data plotted against time on a semilogarithmic diagram. This plot is straight over the first falling period. The slope of this straight line is equal to quantity $\pi^2 D_{\text{eff}}/L^2$ in case of slab geometry.

The effective diffusivity coefficient (D_{eff}) obtained is greater for the red brick samples with pure water than the samples with salt solutions, and the sample with hydraulic continuity interface presents lower values of D_{eff}, as showed in Table 3.

4. Conclusions

In this work an extensive experimental campaign was presented to study the effect of different absorption cycles of two different saturated solutions of sodium sulphate and potassium chloride in the capillary absorption curves obtained through the partial immersion of red brick samples without and with different joints. The drying kinetic process was also analysed for all the samples tested.

The main conclusions were as follows:

(i) Both salts influence the capillary absorption coefficient in a distinct way. The presence of sodium sulphate induces a decrease in this coefficient compared to tests performed with pure water, while the tests performed with potassium chloride showed an increase of the capillary absorption coefficient compared to pure water, despite presenting a lower difference.

(ii) All three types of interface studied presented hydric resistance during the capillary absorption tests, although with different levels of magnitude. Specimens with air space between layers offered much more resistance to moisture transport through their interface compared to both perfect contact and hydraulic contact specimens due to the fact that moisture only flows in vapor phase unlike the other two which also support liquid phase transport.

(iii) Comparing our results with those obtained by de Freitas [12] helped sustaining the author's theory that maximum moisture flow through the air space and perfect contact interfaces (individually) may be fixed within a close range of values for the same material,

Table 3: Values of empirical constants and drying constant for the models tested.

Joints	Solution	Exponential	Page	Logarithmic	Midilli et al.	Diffusional
Monolithic	Water	$k = 1.62 \times 10^{-3}$	$k = 9.24 \times 10^{-3}$ $n = 0.726$	$k = 1.95 \times 10^{-3}$ $a = 0.881$ $b = 9.12 \times 10^{-2}$	$k = 5.96 \times 10^{-3}$ $n = 0.818$ $a = 1.05$ $b = 1.73 \times 10^{-5}$	D_{eff} (m^2/s) = 3.34×10^{-10}
	Water + Na_2SO_4	$k = 3.17 \times 10^{-4}$	$k = 1.03 \times 10^{-3}$ $n = 0.839$	$k = 4.09 \times 10^{-4}$ $a = 0.792$ $b = 0.188$	$k = 6.26 \times 10^{-4}$ $n = 0.903$ $a = 0.985$ $b = 9.47 \times 10^{-7}$	D_{eff} (m^2/s) = $0.48. \times 10^{-10}$
	Water + KCl	$k = 3.75 \times 10^{-4}$	$k = 2.24 \times 10^{-4}$ $n = 1.07$	$k = 3.64 \times 10^{-4}$ $a = 0.986$ $b = 0$	$k = 3.53 \times 10^{-5}$ $n = 1.31$ $a = 0.966$ $b = 0$	D_{eff} (m^2/s) = 0.61×10^{-10}
Hydraulic continuity	Water	$k = 4.14 \times 10^{-4}$	$k = 1.15 \times 10^{-3}$ $n = 0.858$	$k = 5.49 \times 10^{-4}$ $a = 0.842$ $b = 0.156$	$k = 8.72 \times 10^{-4}$ $n = 0.908$ $a = 1.00$ $b = 1.26 \times 10^{-5}$	D_{eff} (m^2/s) = 0.70×10^{-10}
	Water + Na_2SO_4	$k = 4.14 \times 10^{-4}$	$k = 1.26 \times 10^{-3}$ $n = 0.846$	$k = 4.45 \times 10^{-4}$ $a = 0.885$ $b = 8.71 \times 10^{-2}$	$k = 7.65 \times 10^{-4}$ $n = 0.909$ $a = 0.981$ $b = 9.47 \times 10^{-7}$	D_{eff} (m^2/s) = 0.69×10^{-10}
	Water + KCl	$k = 2.51 \times 10^{-4}$	$k = 6.38 \times 10^{-4}$ $n = 0.875$	$k = 3.29 \times 10^{-4}$ $a = 0.783$ $b = 0.203$	$k = 3.53 \times 10^{-5}$ $n = 1.31$ $a = 0.966$ $b = 6.75 \times 10^{-5}$	D_{eff} (m^2/s) = 0.34×10^{-10}
Perfect contact	Water	$k = 2.51 \times 10^{-3}$	$k = 2.77 \times 10^{-2}$ $n = 0.601$	$k = 3.65 \times 10^{-3}$ $a = 0.827$ $b = 0.125$	$k = 4.15 \times 10^{-2}$ $n = 0.545$ $a = 1.06$ $b = 1.48 \times 10^{-6}$	D_{eff} (m^2/s) = 5.08×10^{-10}
	Water + Na_2SO_4	$k = 4.46 \times 10^{-4}$	$k = 1.04 \times 10^{-2}$ $n = 0.559$	$k = 9.15 \times 10^{-4}$ $a = 0.574$ $b = 0.367$	$k = 7.65 \times 10^{-4}$ $n = 0.909$ $a = 0.981$ $b = 5.61 \times 10^{-6}$	D_{eff} (m^2/s) = 0.76×10^{-10}
	Water + KCl	$k = 3.69 \times 10^{-4}$	$k = 3.25 \times 10^{-4}$ $n = 1.02$	$k = 3.57 \times 10^{-4}$ $a = 0.986$ $b = 0$	$k = 8.60 \times 10^{-8}$ $n = 1.19$ $a = 0.973$ $b = 0$	D_{eff} (m^2/s) = 0.59×10^{-10}
Air space interface	Water	$k = 4.30 \times 10^{-3}$	$k = 1.89 \times 10^{-2}$ $n = 0.725$	$k = 5.26 \times 10^{-3}$ $a = 0.907$ $b = 7.31 \times 10^{-2}$	$k = 2.44 \times 10^{-2}$ $n = 0.692$ $a = 1.04$ $b = 1.13 \times 10^{-5}$	D_{eff} (m^2/s) = 8.51×10^{-10}
	Water + Na_2SO_4	$k = 9.77 \times 10^{-4}$	$k = 1.47 \times 10^{-2}$ $n = 0.585$	$k = 1.72 \times 10^{-3}$ $a = 0.693$ $b = 0.261$	$k = 7.77 \times 10^{-4}$ $n = 1.05$ $a = 0.929$ $b = 7.62 \times 10^{-5}$	D_{eff} (m^2/s) = 1.72×10^{-10}
	Water + KCl	$k = 3.99 \times 10^{-4}$	$k = 2.58 \times 10^{-3}$ $n = 0.744$	$k = 6.59 \times 10^{-4}$ $a = 0.686$ $b = 0.284$	$k = 7.48 \times 10^{-4}$ $n = 0.938$ $a = 0.974$ $b = 4.38 \times 10^{-5}$	D_{eff} (m^2/s) = 0.66×10^{-10}

since the maximum moisture flow values determined in this work were very close to the author's for a similar used material.

(iv) Specimens with hydraulic contact interface presented more heterogeneous results. Furthermore this kind of interface's hydric resistance depends on several factors like the water/cement ratio and curing conditions. Despite the difference between the specimen's characteristics, a comparison between ours and Cunha's results shows distinct behaviours in moisture transport through the interface despite using the same cement material.

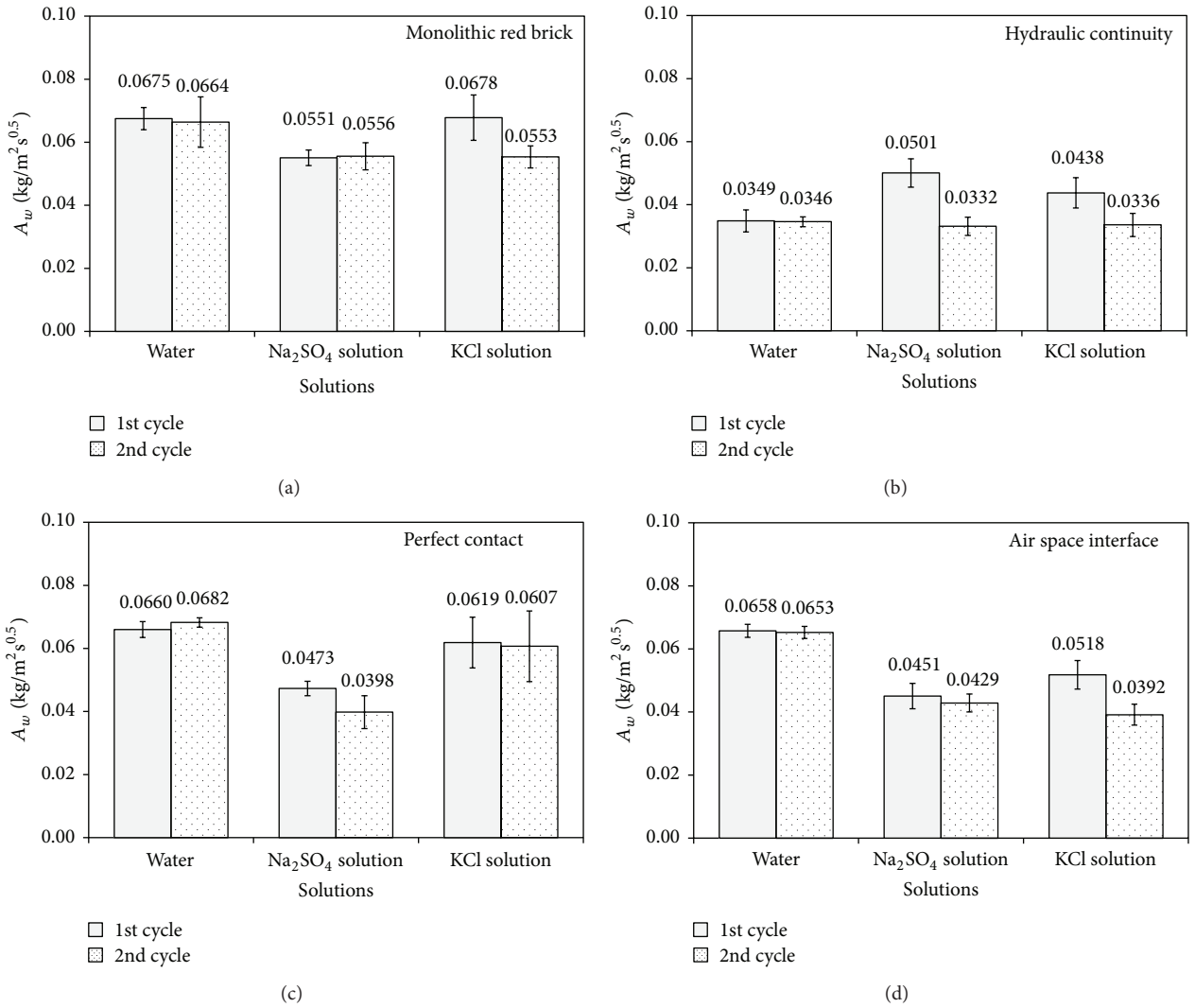

Figure 5: Water absorption coefficient of red brick samples after 1 and 2 cycles, with pure water and saturated solutions of KCl and Na_2SO_4, for (a) monolithic specimens, (b) hydraulic continuity interface, (c) perfect contact interface, and (d) air space interface.

Table 4: Results of the statistical analyses obtained with the drying models tested.

Joints	Solution	Chi-square (χ^2) error				
		Exponential	Page	Logarithmic	Midilli et al.	Diffusional
Monolithic	Water	12.75%	1.54%	5.51%	7.19%	5.93%
	Water + Na_2SO_4	9.01%	1.68%	1.58%	1.10%	20.01%
	Water + KCl	2.28%	2.25%	2.12%	0.86%	11.75%
Hydraulic continuity	Water	1.83%	0.67%	0.60%	0.61%	4.65%
	Water + Na_2SO_4	7.53%	2.23%	2.05%	1.45%	15.90%
	Water + KCl	2.44%	1.46%	0.91%	2.50%	12.66%
Perfect contact	Water	38.75%	4.14%	17.57%	2.76%	14.10%
	Water + Na_2SO_4	73.16%	3.12%	16.67%	57.93%	7.03%
	Water + KCl	1.07%	1.12%	0.89%	0.49%	7.70%
Air space interface	Water	3.93%	1.10%	1.24%	0.54%	2.74%
	Water + Na_2SO_4	69.91%	5.83%	7.69%	18.98%	20.76%
	Water + KCl	8.85%	1.61%	1.04%	1.00%	4.94%
Sum		251.51%	26.75%	57.87%	95.41%	128.17%

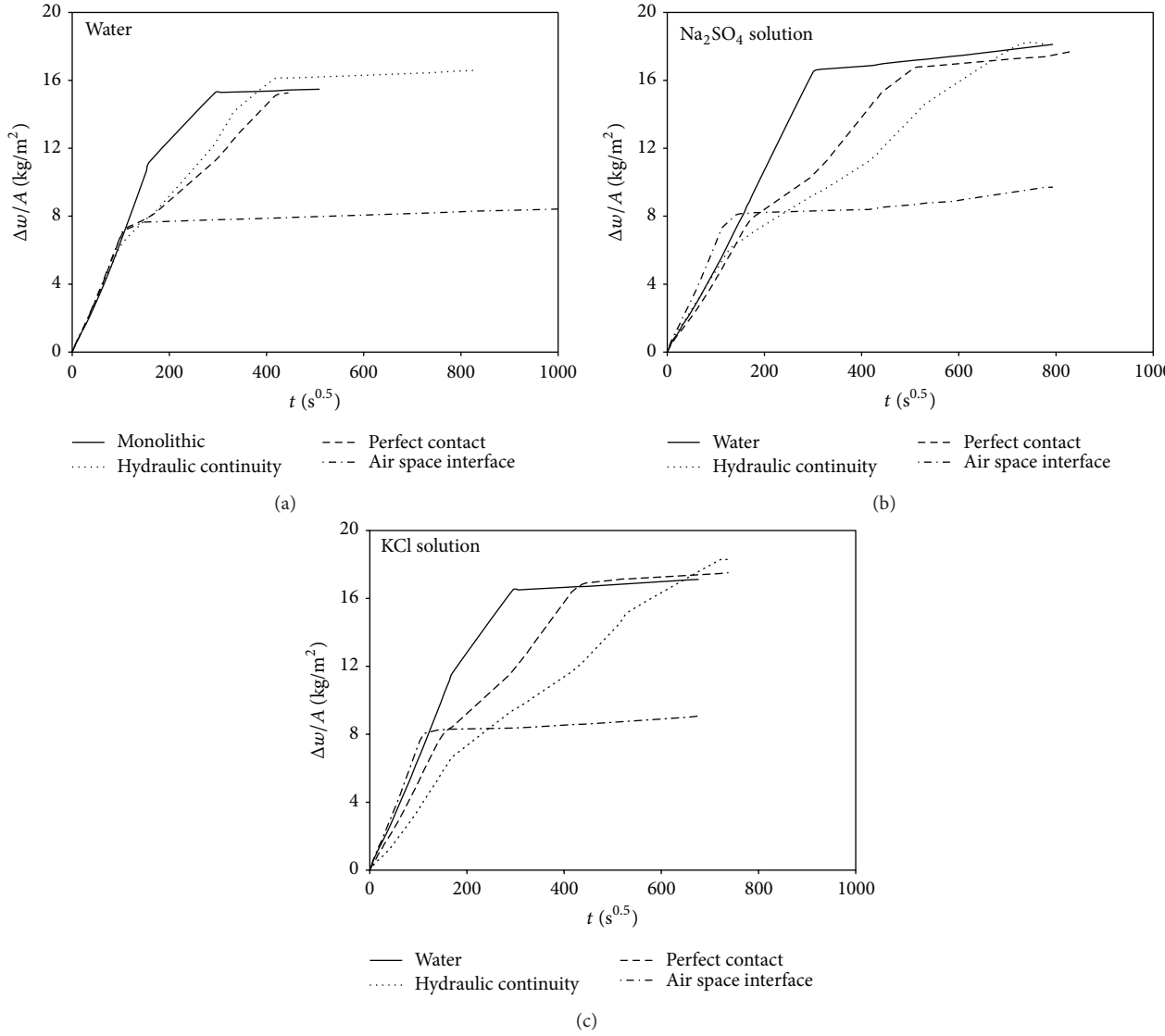

Figure 6: Representation of the absorption in the monolithic specimens and specimens with hydraulic continuity interface, perfect contact interface, and air space interface, for (a) pure water, (b) saturated solution of KCl, and (c) saturated solution of Na_2SO_4.

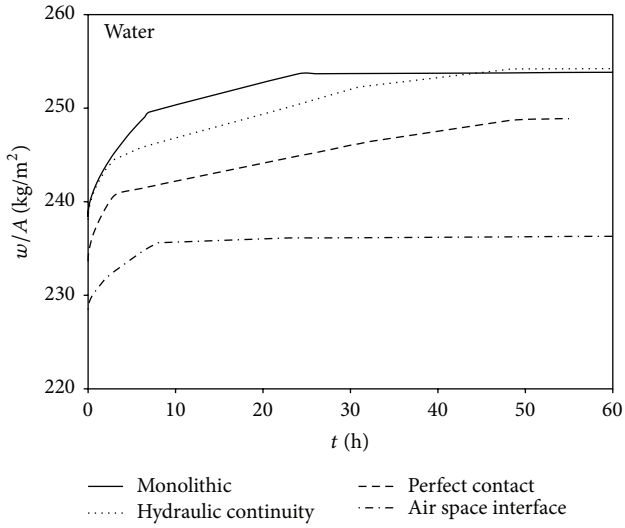

Figure 7: Effect of the different interfaces on the FLUMAX: monolithic specimens, hydraulic continuity interface, perfect contact interface, and air space interface.

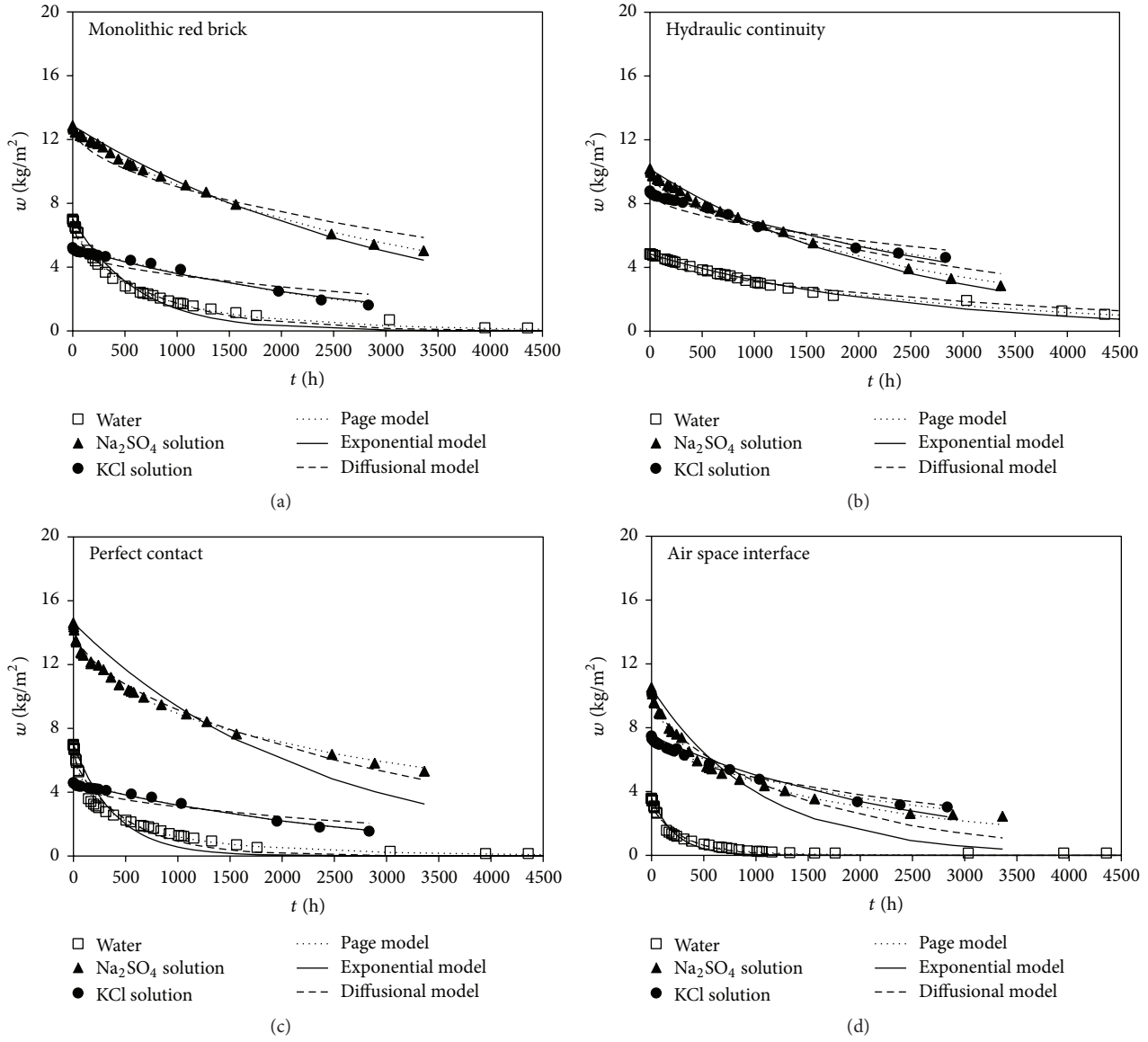

Figure 8: Drying curves of red brick samples with pure water and saturated solutions of KCl and Na_2SO_4, for (a) monolithic specimens, (b) hydraulic continuity interface, (c) perfect contact interface, and (d) air space interface.

(v) Different first-order kinetics models were adjusted to describe the drying process and the results point that the Page and Logarithmic models allow the best fit.

Nomenclature

A: Area
A_w: Capillary absorption coefficient
a, b, n: Empirical coefficients of models
D_{eff}: Effective diffusivity coefficient
k: Drying kinetic coefficient
L: Thickness
MBE: Mean bias error
M_0: Dry mass of the sample
M_i: Mass of sample at time
M_w: Amount of absorbed water per unit area
MR: Moisture ratio, $\text{MR} = (w - w_{\text{eq}})/(w_0 - w_{\text{eq}})$
N: Number of experimental points
p: Number of estimated parameters
RMSE: Root mean square error
S: Sorptivity
t: Time
T: Temperature
x: Axial coordinate
w: Moisture content
w_e: Equilibrium moisture content
w_0: Initial moisture content
χ^2: Chi-square test
ρ_w: Water density.

Competing Interests

The authors declare that they have no competing interests.

Acknowledgments

The authors acknowledge the Foundation for Science and Technology (FCT) for the financial support (PTDC/ECM-COM/3080/2012). J. M. P. Q. Delgado would like to thank FCT for financial support through the Grant SFRH/BPD/109310/2015.

References

[1] A. S. Guimarães, J. M. Q. Delgado, and V. P. de Freitas, "Rising damp in walls: evaluation of the level achieved by the damp front," *Journal of Building Physics*, vol. 37, no. 1, pp. 6–27, 2013.

[2] A. S. Guimarães, J. M. P. Q. Delgado, and V. P. de Freitas, "Rising damp in building walls: the wall base ventilation system," *Heat and Mass Transfer*, vol. 48, no. 12, pp. 2079–2085, 2012.

[3] H. S. Hens, *Building Physics-Heat, Air and Moisture-fundamentals and Engineering Methods with Examples and Exercises*, Ernst & Sohn, Brussels, Belgium, 2007.

[4] C. Hall, "Water sorptivity of mortars and concretes: a review," *Magazine of Concrete Research*, vol. 41, no. 147, pp. 51–61, 1989.

[5] R. J. Gummerson, C. Hall, and W. D. Hoff, "Water movement in porous building materials-III. A sorptivity test procedure for chemical injection damp proofing," *Building and Environment*, vol. 16, no. 3, pp. 193–199, 1981.

[6] C. Hall and W. D. Hoff, *Water Transport in Brick, Stone and Concrete*, Taylor & Francis, London, UK, 2002.

[7] J. M. P. Q. Delgado, N. M. M. Ramos, and V. P. de Freitas, "Can moisture buffer performance be estimated from sorption kinetics?" *Journal of Building Physics*, vol. 29, no. 4, pp. 281–299, 2006.

[8] L. Pel, H. Huinink, and K. Kopinga, "Salt transport and crystallization in porous building materials," *Magnetic Resonance Imaging*, vol. 21, no. 3-4, pp. 317–320, 2003.

[9] D. Young, *Salt Attack and Rising Damp: A Guide to Salt Damp in Historic and Older Buildings*, Heritage Council of NSW, Heritage Victoria, South Australian, Adelaide City Council, 2008.

[10] T. Gonçalves, *Salt crystallization in plastered or rendered walls [Ph.D. thesis]*, Technical University of Lisbon and LNEC, Lisbon, Portugal, 2007.

[11] J. Azevedo, *Capillary absorption of porous materials in salt solutions [M.S. thesis]*, Faculty of Engineering, University of Porto, Porto, Portugal, 2013.

[12] V. P. de Freitas, *Moisture transfer in building walls—interface phenomenon analyse [Ph.D. thesis]*, Faculty of Engineering, University of Porto, Porto, Portugal, 1992.

[13] A. S. Guimarães, J. M. P. Q. Delgado, and V. P. de Freitas, "Influence of mortar joints on the moisture transfer in layered materials," *Defect and Diffusion Forum*, vol. 365, pp. 160–165, 2015.

[14] H. Derluyn, H. Janssen, and J. Carmeliet, "Influence of the nature of interfaces on the capillary transport in layered materials," *Construction and Building Materials*, vol. 25, no. 9, pp. 3685–3693, 2011.

[15] RILEM TC 25-PEM, "Recommended tests to measure the deterioration of stone and to assess the effectiveness of treatment methods," *Materials and Structures*, vol. 13, pp. 204–209, 1980.

[16] P. Mukhopadhyaya, K. Kumaran, N. Normandin, and P. Goudreau, "Effect of surface temperature on water absorption coefficient of building materials," *Journal of Thermal Envelope and Building Science*, vol. 26, no. 2, pp. 179–195, 2002.

[17] H. A. Iglesias and J. Chirife, *Handbook of Food Isotherms*, Academic Press, New York, NY, USA, 1983.

[18] D. Marinos-Kouns, Z. B. Maroulis, and C. T. Kiranoudis, "Computer simulation of industrial dryers," *Drying Technology*, vol. 14, no. 5, pp. 971–1010, 1996.

[19] J. Crank, *The Mathematics of Diffusion*, Oxford University Press, Oxford, UK, 2nd edition, 1975.

[20] J. M. P. Q. Delgado, N. M. M. Ramos, E. Barreira, and V. P. de Freitas, "A critical review of hygrothermal models used in porous building materials," *Journal of Porous Media*, vol. 13, no. 3, pp. 221–234, 2010.